Effect of Substituents on the Strength of A−Cl^- (A = Si, Ge, and Sn) Bonds in Hypervalent Systems: ACl_5^-, ACl_4F^-, and $A(CH_3)_3Cl_2^-$

Changtong Hao, Jennifer D. Kaspar, Catherine E. Check, Kim C. Lobring, Thomas M. Gilbert, and Lee S. Sunderlin*

Department of Chemistry and Biochemistry, Northern Illinois University, DeKalb Illinois 60115

Received: December 3, 2004

The gas-phase strengths of the A−Cl^- bonds in ACl_5^-, ACl_4F^-, and $A(CH_3)_3Cl_2^-$ (A = Si, Ge, and Sn) have been determined by measuring thresholds for collision-induced dissociation in a flowing afterglow-tandem mass spectrometer. Bond dissociation energies increase in the order Si < Ge < Sn. Replacement of the three equatorial chlorides with methyl groups weakens the bonds, while replacing one axial chloride with a fluoride strengthens the bonds. Computational results using the B3LYP model with several basis sets parallel the experimental periodic trends, but provide bond dissociation energies lower than experiment by 7−44 kJ mol^{-1}. MP2 computational results are in better agreement with experiment. The results are consistent with steric hindrance and electrostatic effects playing significant roles in the bonding energetics.

Introduction

Group 14 tetrahalides AX_4 (A = Si, Ge, Sn; X = F, Cl, Br, and I) are Lewis acids; they react with halide anions to form pentacoordinate AX_5^- complexes[1−4] with 10 electrons around the central atom. Pentacoordinate complexes serve as reactive intermediates in nucleophilic substitution reactions of tetracoordinate silicon species and in the transformation from tetra- to hexacoordinate silicon complexes.[5] Unexpectedly, the pentacoordinate species are more reactive toward nucleophiles such as Grignard reagents than tetracoordinate silicon complexes.[6] Pentacoordinate species involving group 14 elements are also found as intermediates in S_N2 reactions. For example, oxidative addition to $(CH_3)_3SnCl$ proceeds through a five-coordinate tin complex.[7] The thermochemistry of pentacoordinate complexes can be helpful in understanding the kinetics and dynamics of these reactions. The energetics of addition to group 14 complexes can be substantially affected by differential solvation of the reactants and the products;[8] measurements of the gas-phase thermochemistry of five-coordinate complexes allow the effects of solvation to be determined.

The AX_5^- complexes are trigonal bipyramids with two axial ligands and three equatorial ligands. The gas-phase X_4A-X^- bond dissociation energies (BDEs) are a direct measure of the Lewis acidity of AX_4 in the absence of solvent effects. Previous work has indicated that Lewis acidity increases in the order Si < Ge < Sn.[9−11] This work reports measurements of the Cl_4A-Cl^- BDEs to determine the effect of changing the central group 14 element, A, on the BDE. The X_4A-X^- BDEs also reflect the influence of the axial A−X bond trans to the broken bond, as well as the three equatorial A−X bonds. Therefore, we have measured BDEs in $A(CH_3)_3Cl_2^-$ and ACl_4F^- to determine the effects of substitution of the equatorial ligands and axial ligand on the A−Cl^- BDE. Computational studies of the systems examined experimentally, as well as related systems with mixed equatorial ligands, are also discussed.

Although no systematic examination of the effects of other ligands on gas-phase BDEs in group 14-based systems have been reported, the results of several previous studies are relevant to the present work. Larson and McMahon[12,13] measured an extensive set of chloride and fluoride affinities, which provide additional insight into the issues addressed here. This work will be discussed further below.

Previous computational work relevant to this study includes a study[14] by Gordon and co-workers on pseudorotation in $SiCl_5^-$ and related molecules that utilized MP2 and MP4 methods; they noted that lower levels of theory were not qualititively accurate on this type of system. Alkorta et al. performed an extensive study of the bonding in neutral $SiCl_4$-X complexes[15] using MP2 and B3LYP[16] methods. Fleischer studied a range of substituted silane−Lewis base complexes with density functional methods similar to those employed here.[17] Halogenated four-coordinate silicon compounds have been studied using very high-level techniques by Chien, Li, and Ma.[18]

Experimental Section

BDEs were measured using the energy-resolved collision-induced dissociation (CID) technique[19,20,21] in a flowing afterglow-tandem mass spectrometer (MS).[22] The instrument consists of an ion source region, a flow tube, and the tandem MS. The dc discharge ion source used in these experiments is typically set at 2000 V with 2 mA of emission current. The flow tube is a 92 cm × 7.3 cm i.d. stainless steel pipe that operates at a buffer gas pressure of 0.35 Torr, a flow rate of 200 standard cm^3 s^{-1}, and an ion residence time of 100 ms. The buffer gas is helium with up to 10% argon added to stabilize the dc discharge.

To make ACl_5^- for this study, ACl_4 was added to the ion source. Dissociative electron impact gives Cl^-, which adds to a further molecule of ACl_4 to give ACl_5^-. Approximately 10^5 collisions with the buffer gas cool the metastable ACl_5^- ions to room temperature. C_2Cl_4 was added as an additional Cl^- source. ACl_4F^- ions were produced with the addition of SF_6 instead of C_2Cl_4 to the flow tube; $A(CH_3)_3Cl_2^-$ ions were produced from C_2Cl_4 and $A(CH_3)_3Cl$. All precursors except SF_6 were cooled in an ice bath to improve control of the vapor flow.

The tandem MS includes a quadrupole mass filter, an octopole ion guide, a second quadrupole mass filter, and a detector,

* Corresponding author: E-mail: sunder@niu.edu 815-753-6870.

10.1021/jp040743x CCC: $30.25
Published on Web 02/12/2005

contained in a stainless steel box that is partitioned into five interior chambers. Differential pumping on the five chambers ensures that further collisions of the ions with the buffer gas are unlikely after ion extraction. During CID experiments, the ions are extracted from the flow tube and focused into the first quadrupole for mass selection. The reactant ions are then focused into the octopole, which passes through a reaction cell that contains an unreactive collision gas. Xe was used for most of the anions in this study, but Ar was used with $Si(CH_3)_3Cl_2^-$ and $Ge(CH_3)_3Cl_2^-$. With the present instrumentation, use of Ar as the collision gas gives more precise results for ions that are light and have low BDEs; these two ions fulfill these criteria. After the dissociated and unreacted ions pass through the reaction cell, the second quadrupole is used for mass analysis. The detector is an electron multiplier operating in pulse-counting mode.

The energy threshold for CID is determined by modeling the cross section for product formation as a function of the reactant ion kinetic energy in the center-of-mass (CM) frame, E_{cm}. The octopole is used as a retarding field analyzer to measure the reactant ion beam energy zero. The ion kinetic energy distribution for the present data is typically Gaussian with a full-width at half-maximum of 0.5−2.0 eV (1 eV = 96.5 kJ mol^{-1}). The octopole offset voltage measured with respect to the center of the Gaussian fit gives the laboratory kinetic energy, E_{lab}, in eV. Low offset energies are corrected for truncation of the ion beam.[23] To convert to the center-of-mass (CM) frame, the equation $E_{cm} = E_{lab}m(m + M)^{-1}$ is used, where m and M are the masses of the neutral and ionic reactants, respectively. All experiments were performed with both mass filters at low resolution to improve ion collection efficiency and reduce mass discrimination. Average atomic masses were used for all elements.

The total cross section for a reaction, σ_{total}, is calculated using eq 1, where I is the intensity of the reactant ion beam, I_o is the intensity of the incoming beam ($I_o = I + \Sigma I_i$), I_i is the intensity of each product ion, n is the number density of the collision gas, and l is the effective collision length, 13 ± 2 cm. Individual product cross sections σ_i are equal to σ_{total} ($I_i/\Sigma I_i$).

$$I = I_o \exp(-\sigma_{total} n l) \quad (1)$$

Threshold energies are derived by fitting the data to a model function given in eq 2, where $\sigma(E)$ is the cross section for formation of the product ion at center-of-mass energy E, E_T is the desired threshold energy, σ_o is the scaling factor, n is an adjustable parameter, and i denotes rovibrational states having energy E_i and population g_i ($\Sigma g_i = 1$). Doppler broadening and the kinetic energy distribution of the reactant ion are also accounted for in the data analysis, which is done using the CRUNCH program written by P. B. Armentrout and co-workers.

$$\sigma(E) = \sigma_o \Sigma_i g_i (E + E_i - E_T)^n / E \quad (2)$$

Collisionally activated metastable complexes can have sufficiently long lifetimes that they do not dissociate on the experimental time scale (ca. 50 μs). Such kinetic shifts are accounted for in the CRUNCH program by RRKM lifetime calculations. Reactant and product vibrational frequencies are needed to determine both the RRKM lifetimes and the reactant internal energy distribution.

Complete experimental fundamental vibrational frequency sets are available for the neutral ACl_4 molecules, and nearly complete sets are available for the ACl_5^- anions.[24] However, only limited results are available for the trimethyl and fluorine-containing species,[25] such that the dissociation modeling described above cannot be performed using solely experimental data. Therefore, vibrational harmonic frequencies and rotational constants were calculated using the Kohn−Sham DFT method with the B3LYP functional to give a consistent set of frequencies for all analyses. Several basis sets were used. The 6-311+G(d) basis set[26] was used for all of the Si- and Ge-containing species, but this basis set is not available for tin. The aug-cc-pVTZ basis set[27] was used for the silicon and germanium chlorides and fluorochlorides, and the SDB-aug-cc-pVTZ basis set[28] (which uses the SDB effective core for tin) was used for the corresponding tin compounds. The smaller LANL2DZpd basis set,[29,30] which uses the LANL effective core potential, was used for all of the molecules involved in this study. The calculated frequencies are given in the Supporting Information. The frequencies determined using all three basis sets are lower than the known experimental values by 2−7%, results typical for this type of system.[30,31] Other work on closely related molecules with the 6-311+G(d, p) basis set and the aug-cc-pVTZ basis set suggest that these basis sets give generally good agreement with experiment without scaling.[32] Because the derived thermochemistry is most sensitive to the *ratio* of the reactant and product frequencies, unscaled computational results were used for all molecules. 6-311+G(d) results were used for Si- and Ge-containing species, and LANL2DZpd results were used for Sn-containing species.

Uncertainties in the derived thresholds due to possible inaccuracies in the frequencies were estimated by multiplying the entire sets of frequencies by 0.9 and 1.1, and by multiplying the time window for dissociation by 10 and 0.1. The effect of this scaling on the calculated thresholds is 1−3 kJ mol^{-1} for the pentahalide anions and up to 6 kJ mol^{-1} for the trimethyl species. Polarizabilities for neutral molecules were also taken from the computational results; varying these parameters has a negligible effect on the derived BDEs.

An ion not sufficiently energized by one collision with the target gas may gain enough energy in a second collision to exceed the dissociation threshold. This effect is eliminated by linear extrapolation of the data taken at several pressures to a zero pressure cross section before fitting the data.[33]

The reagents $Si(CH_3)_3Cl$, $Ge(CH_3)_3Cl$, $Sn(CH_3)_3Cl$, $SiCl_4$, $GeCl_4$, and $SnCl_4$ were obtained from Acros. He, Ar, and SF_6 were obtained from BOC, and Xe was obtained from Spectra Gases. All reagents were used as received.

The effects on BDEs of mixed sets of equatorial ligands is difficult to address experimentally. One difficulty is the overlap of the mass distributions of many five-coordinate ions with radical anions. For example, $A(CH_3)_2Cl_3^-$ and $AF_2Cl_3^-$ have mass distributions that overlap with that of ACl_4^-, which is formed in the ions source. This makes it difficult to determine the cross section for chloride loss from the pentacoordinate ion. However, computations on the intermediate systems $A(CH_3)Cl_4^-$ and $A(CH_3)_2Cl_3^-$ were performed in addition to work on the systems studied experimentally.

Computational Details. Most of the computational work on these systems was performed using the Gaussian 98 Suite.[34] All molecular structures were optimized without symmetry constraints, and plausible alternative structures were tested. The nature of all stationary point structures were determined by analytical frequency analysis, which also provided zero-point energies (ZPEs). As was true for the frequencies above, the ZPEs were not scaled when used to correct the raw energy values. The natural bond orbitals analysis (NBO)[35] program was also used to study the charge distributions in these systems.

TABLE 1: Fitting Parameters for CID[a]

anion	E_T(eV)	n
$SiCl_5^-$	1.09 ± 0.06	1.1 ± 0.1
$SiCl_4F^-$	1.18 ± 0.04	1.2 ± 0.1
$Si(CH_3)_3Cl_2^-$	0.63 ± 0.05	1.1 ± 0.1
$GeCl_5^-$	1.46 ± 0.02	1.0 ± 0.1
$GeCl_4F^-$	1.72 ± 0.04	1.0 ± 0.1
$Ge(CH_3)_3Cl_2^-$	0.97 ± 0.04	1.0 ± 0.1
$SnCl_5^-$	2.42 ± 0.06	1.1 ± 0.1
$SnCl_4F^-$	2.60 ± 0.10	1.0 ± 0.1
$Sn(CH_3)_3Cl_2^-$	1.36 ± 0.07	1.0 ± 0.1

[a] See text for discussion of fitting parameters.

Additional "pure" DFT calculations and geometry optimizations were carried out using the Amsterdam density functional (ADF) program[36] developed by Baerends et al.[37] and vectorized by Ravenek.[38] The numerical integration scheme applied for the calculations was developed by te Velde et al.;[39] the geometry optimization procedure derives from that of Versluis and Ziegler.[40] Geometry optimizations were carried out using the local density approximation of Vosko, Wilk, and Nusair (LDA VWN)[41]augmented with the nonlocal gradient correction PW91 from Perdew and Wang.[42] Relativistic corrections were added using a scalar-relativistic zeroth order relativistic approximation (ZORA) Hamiltonian.[43,44] The electronic configurations of the molecular systems were described by a triple-ζ + polarization (TZP) basis set for all atoms. Non-hydrogen atoms were assigned a relativistic frozen core potential, treating as core the shells up to and including: 1s for C and F, 2p for Si and Cl, 3p for Ge, and 4p for Sn. A set of auxiliary s, p, d, and f functions, centered on all nuclei, was used to fit the molecular density and represent Coulomb and exchange potentials accurately in each SCF cycle.

The large number of systems investigated and the computational effort required to calculate second derivatives of the energy with respect to the nuclear positions make ZPE corrections using the ADF program prohibitive. ZPE corrections lower the BDEs in the systems studied by 1−3 kJ mol^{-1}; the omission of this effect has little impact on the bond decomposition energy data.

Results and Discussion

Computed Geometries. The optimized geometries are very similar for all basis sets employed. Calculated bond lengths between the nonhydrogen atoms are given in Table 3. All of the anions studied in this work have five ligands around the central atom and trigonal bipyramidal (TBP) geometries, although there are small distortions from the ideal geometries for the $AFCl_4^-$ systems. The neutral products are all calculated to have nearly tetrahedral geometries around the central atom. (In this discussion, the hydrogen atoms in methyl groups are neglected because they are not directly involved in the bonding of interest.) Calculations on the different structural isomers indicate that the fluorine atoms in ACl_4F^- and $ACl_3F_2^-$ are apical, and the chlorine atoms in $A(CH_3)_3Cl_2^-$ are apical, in agreement with expectations.[45−47] Similarly, crystallographic analysis of SiF_5^-, $PhSiF_4^-$, and $Ph_2SiF_3^-$ show geometries close to TBP, in which the organic groups occupy equatorial positions.[48]

Relatively few of the calculated bond lengths can be compared to experimental values. Many of the compounds studied here, such as $(CH_3)_3SnCl$, form 5- or 6-coordinated polymers in the crystalline state.[49] The crystal structure of $PPh_4^+SnCl_5^-$ has been determined, but the structure is noticeably distorted from TBP symmetry.[50] A few gas-phase measurements have been carried out.[51,52] These results are summarized in Table 3. The calculated values are 2−5 pm longer than the gas-phase experimental values, consistent with the B3LYP method tending to give slightly long bond lengths.[53]

Bond lengths in the systems studied depend on the central atom: bonds to Ge are longer than bonds to Si by 8−14 pm, while bonds to Sn are longer than bonds to Ge by 9−18 pm. Substitution of an axial chlorine in ACl_5^- with a fluorine atom has almost no effect on either the equatorial or the remaining axial A−Cl bond lengths (≤0.014 Å). The F−A−Cl_{eq} bond angles in the $AFCl_4^-$ complexes are slightly smaller than 90°, consistent with axial chlorine ligands having greater steric influence than fluorine ligands.

Experimental Bond Dissociation Energies. The CID of all species studied in this work gives loss of Cl^- as the dominant dissociation pathway. Loss of neutral Cl_2 and Cl atom were also observed at high energies for the ACl_5^- and ACl_4F^- ions, but the cross sections for these processes are less than 1% of the cross section for chloride loss in the reaction threshold region. Thus, the minor products are not considered further in this work.

Appearance curves for dissociation of $SiCl_5^-$, $Ge(CH_3)_3Cl_2^-$, and $SnCl_4F^-$ are given in Figures 1−3, and they are representative of the data for all systems examined here. The other six appearance curves are given in the Supporting Information. The eq 2 fitting parameters for all nine systems are given in Table 1, and the fits are shown in the figures. The effects of reactant and product internal energy are included in the fitting procedure;

TABLE 2: A−Cl$^-$ (A = Si, Ge, Sn) Bond Dissociation Enthalpies in kJ mol^{-1}

anion	expt (0 K)	expt (298 K)	B3LYP/6-311+G(d)	B3LYP/LANL2DZpd	B3LYP/aug-cc-pVTZ	MP2/LANL2DZpd	PW91/TZP
$Si(CH_3)_3Cl_2^-$	60 ± 6	60 ± 6	49.3	47.1	49.1	78.2	80.9
$Si(CH_3)_2Cl_3^-$			52.2	53.1	52.7	82.6	
$Si(CH_3)Cl_4^-$			60.0	65.0	61.4	89.0	
$SiCl_5^-$	105 ± 8	105 ± 8	81.9	89.5	83.8	104.6	116.2
$SiCl_4F^-$	114 ± 7	115 ± 7	95.1	105.1	89.0	117.1	124.9
$Ge(CH_3)_3Cl_2^-$	94 ± 6	93 ± 6	76.9	78.1	74.8	108.7	102.9
$Ge(CH_3)_2Cl_3^-$	−	−	84.2	86.7	81.0	114.8	
$Ge(CH_3)Cl_4^-$	−	−	93.9	99.7	90.0	122.9	
$GeCl_5^-$	140 ± 6	141 ± 6	125.1	133.1	118.0	145.3	149.5
$GeCl_4F^-$	166 ± 7	167 ± 7	147.0	150.9	134.3	167.3	166.3
$Sn(CH_3)_3Cl_2^-$	131 ± 7	131 ± 7		124.1	120.7	141.4	145.9
$Sn(CH_3)_2Cl_3^-$				130.7	130.1	162.2	
$Sn(CH_3)Cl_4^-$				162.8	153.4	189.3	
$SnCl_5^-$	234 ± 8	235 ± 8		190.9	190.4	221.2	220.8
$SnCl_4F^-$	250 ± 12	251 ± 12		217.8	206.6	236.1	237.1
rms[a]			17.7	21.0	27.8	10.8	12.5

[a] Rms = $[\Sigma(E_{calc} - E_{exp})^2/n]^{1/2}$, where n is the number of values compared.

TABLE 3: Structural Data for ACl_5^-, ACl_4F^-, and $A(CH_3)_3Cl_2^-$ Anions and Chloride Loss Products (A = Si, Ge, Sn)[a]

molecule	r_{ax}(A−Cl)	r_{eq}(A−Cl)	∠Cl_{ax}−A−Cl_{eq}	r(Cl−Cl)
$SiCl_5^-$	2.247	2.130	90.0	3.095
$GeCl_5^-$	2.332	2.235	90.0	3.230
$SnCl_5^-$	2.450	2.398	90.0	3.428
expt[b]	2.391	2.339 (×2), 2.293	88.7−92.0	

molecule	r_{ax}(A−Cl)	r_{ax}(A−F)	r_{eq}(A−Cl)	∠F−A−Cl_{eq}	r(Cl−Cl)	r(Cl−F)
$SiFCl_4^-$	2.242	1.659	2.144	89.8	3.106	2.707
$GeFCl_4^-$	2.330	1.797	2.236	89.2	3.251	2.849
$SnFCl_4^-$	2.447	1.959	2.393	88.9	3.454	3.064

molecule	r_{ax}(A−Cl)	r_{eq}(A−C)	∠Cl−A−C_{eq}
$Si(CH_3)_3Cl_2^-$	2.486	1.892	90.0
$Ge(CH_3)_3Cl_2^-$	2.571	1.971	90.0
$Sn(CH_3)_3Cl_2^-$	2.654	2.147	90.0

molecule	r(A−Cl)	∠Cl−A−Cl	r(Cl−Cl)
$SiCl_4$	2.045	109.5	3.339
expt[c]	2.02		3.28
$GeCl_4$	2.141	109.5	3.496
expt[c]	2.11		3.45
$SnCl_4$	2.316	109.5	3.781
expt[c]	2.28		3.72

molecule	r(A−Cl)	r(A−F)	∠F−A−Cl	F−Cl	Cl−Cl
$SiFCl_3$	2.036	1.591	108.2	3.351	2.949
$GeFCl_3$	2.130	1.722	107.5	3.116	3.517
$SnFCl_3$	2.306	1.899	107.6		

molecule	r(A−Cl)	r(A−C)	∠Cl-A−C
$Si(CH_3)_3Cl$	2.112	1.876	107.1
$Ge(CH_3)_3Cl$	2.223	1.961	105.6
$Sn(CH_3)_3Cl$	2.393	2.137	105.2
expt[d]	2.354	2.108	103.2

[a]Key: eq = equatorial; ax = axial. Distances are in Å, angles in degrees. Values were calculated using the B3LYP method and the aug-cc-pVTZ basis set for all atoms except Sn, where the SDB-aug-cc-pVTZ basis set is used. Double degeneracy denoted by (×2). [b] Reference 50. [c] Reference 51. [d] Reference 52.

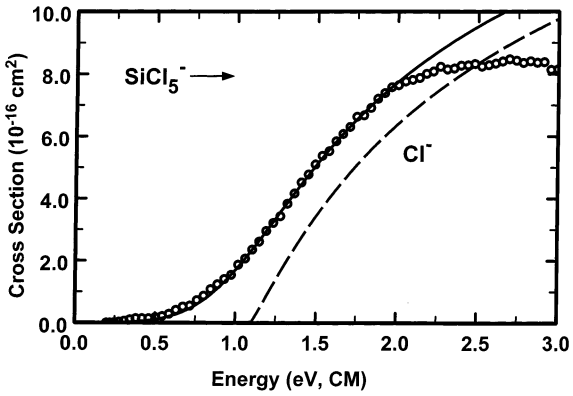

Figure 1. Cross section for collision-induced dissociation of $SiCl_5^-$ as a function of energy in the center-of-mass frame. The solid and dashed lines represent convoluted and unconvoluted fits to the data, as discussed in the text.

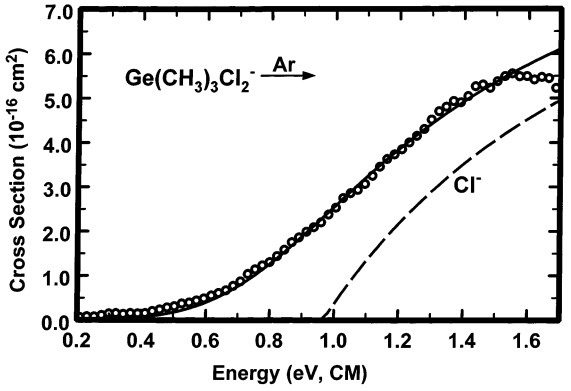

Figure 2. Cross section for collision-induced dissociation of $Ge(CH_3)_3Cl_2^-$ as a function of energy in the center-of-mass frame. The solid and dashed lines represent convoluted and unconvoluted fits to the data, as discussed in the text.

therefore, the dissociation thresholds correspond to BDEs at 0 K. The final uncertainties in the BDEs are derived from the standard deviation of the thresholds determined for individual data sets, the uncertainty in the reactant internal energy, the effects of kinetic shifts, and the uncertainty in the energy scale (±0.15 eV lab). These results are given in Table 2.

The relative locations of the solid and dashed lines are different in these three figures, but the reasons are straightforward. The dashed lines (unconvoluted fits) represent the cross sections expected if the reactant ions had no internal energy, there was no energy broadening, and the activated ions always dissociated if given sufficient energy. The solid lines (convoluted fits) include the effect of ion internal energy, broadening, and delayed dissociation, as discussed above. For $SiCl_5^-$, the main effect is the internal energy of the ion (0.20 eV on average), which shifts the solid line to the left. $Ge(CH_3)_3Cl_2^-$ has more degrees of freedom and more internal energy (0.28 eV), resulting in a larger difference between the convoluted and unconvoluted fits. For $SnCl_4F^-$, the higher BDE leads to a significantly large kinetic shift, nearly canceling the effect of the internal energy.

The experimental 0 K BDEs are converted into 298 K bond enthalpies using the integrated heat capacities of the reactants

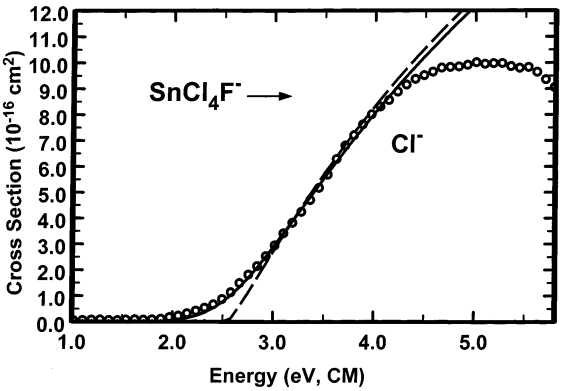

Figure 3. Cross section for collision-induced dissociation of $SnCl_4F^-$ as a function of energy in the center-of-mass frame. The solid and dashed lines represent convoluted and unconvoluted fits to the data, as discussed in the text.

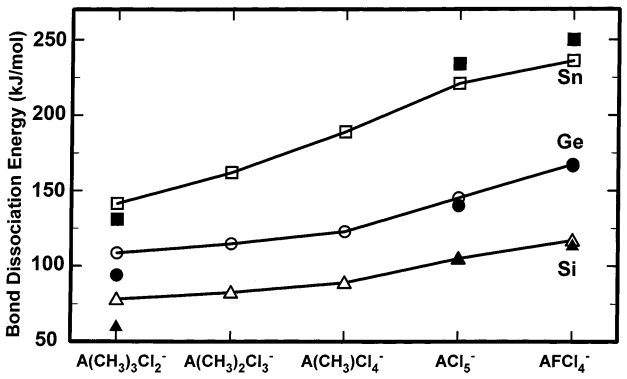

Figure 4. Experimental and computational (MP2/LANL2DZpd) bond dissociation energies for group 14 anions at 0 K. Close symbols represent experimental values. Open symbols and lines represent calculated values.

and products. The heat capacities were determined using the calculated frequencies. The thermal corrections for these systems are small, such that the bond enthalpies change by 1 kJ mol^{-1} or less (Table 2). One of the 298 K values can be compared to a previous experimental determination. The value measured here for $SiCl_5^-$, $D_{298}(SiCl_4-Cl^-) = 105 \pm 8$ kJ mol^{-1}, is in good agreement with the value previously measured by Larson and McMahon, 101 kJ mol^{-1}.

Computational Bond Dissociation Energies. BDEs calculated at various levels of theory are summarized in Table 2. The MP2 results are in generally good agreement with experiment for the ACl_5^- and ACl_4F^- systems but are higher than the experimental values for $A(CH_3)_3Cl_2^-$. Overall, this model provides the best agreement of those tested, with an RMS error of 11 kJ mol^{-1}, about half that observed for the B3LYP approaches. $D(SiCl_4-Cl^-)$ was previously calculated to be 92 kJ mol^{-1} at the MP4/6-31+G(d)//MP2/6-31+G(d) level, in reasonable agreement with the experimental value and the MP2/LANL2DZpd value (both 105 kJ mol^{-1}). The B3LYP BDEs are consistently lower than experimental values, with RMS deviations of 18−28 kJ mol^{-1}. Of the three basis sets used with the B3LYP model, the LANL2DZpd basis set typically gives the highest (and most accurate) BDEs, while aug-cc-pVTZ gives the lowest (and least accurate). The basis set dependence is not very large, with an average range of 10 kJ mol^{-1} for each molecule. The deviations tend to be larger for fluoride-containing anions than for methyl-containing anions.

Periodic Trends in Bond Dissociation Energies. Several trends are apparent in the BDEs. For all three ligand sets, the BDEs increase in the order Si < Ge < Sn; this ordering of Lewis acidity has also been noted in solution. The agreement of gas-phase and solution trends is consistent with the predictions of the Born model,[54] which states that solvation free energies for ions are inversely proportional to the ionic radius. For water at room temperature, $\Delta_{sol}G$ equals 686 kJ mol^{-1} divided by the ionic radius in angstroms. Because smaller ions have greater solvation energies, and the radii of the AL_4Cl^- (L = ligand) ions are much larger than the radius of Cl^-, solution-phase chloride affinities are smaller than gas-phase chloride affinities. The solvation energy is 365 kJ mol^{-1} for Cl^-.[55] The volumes of the AL_4Cl^- ions were estimated using Gaussian 98 and the B3LYP/LANL2DZpd method. The results give volumes of 90−110 Å^3, leading to $\Delta_{sol}G = 230-250$ kJ mol^{-1}. Assuming the entropy differences are small, the solvation enthalpies are nearly the same for the complexes discussed in this work. The relatively narrow range of volumes for the five-coordinated anions explains the similarity in the observed trends in the gas phase and solution.

Theory and experiment agree that the BDEs follow the order $D(AFCl_3-Cl^-) > D(ACl_4-Cl^-) > D(A(CH_3)_3Cl-Cl^-)$. Figure 4 shows the trends in the experimental and MP2/LANL2DZpd BDEs. The increase in stability with increasing numbers of fluoride ligands has been previously noted for germanium pentahalides. The decrease in Lewis acidity upon methyl group substitution for chlorine in $SnCl_4$ was also previously observed in solution.[56]

Extensive scales of relative fluoride and chloride affinities were measured by Larson and McMahon. Fluoride results that relate to the present experiments include $D(Si(CH_3)_4-F^-) = 125$ kJ mol^{-1}, $D(Si(CH_3)_3F-F^-) = 192$ kJ mol^{-1}, $D(Si(CH_3)F_3-F^-) = 243$ kJ mol^{-1}, and $D(SiF_4-F^-) \geq D(ClH-F^-) = 250$ kJ mol^{-1}.[12,57] The trends in these bond enthalpies parallel the present results: more electronegative equatorial or axial ligands increase the axial bond strength. Previous calculations on pentacoordinate silicon compounds agree that more electronegative equatorial substituents increase the axial bond strength, an effect attributed to greater electrostatic interactions.[58]

Larson and McMahon also reported a set of chloride affinities, including $D(SiCl_4-Cl^-) = 101$ kJ mol^{-1}, $D(SiF_4-Cl^-) = 98$ kJ mol^{-1}, and $D(Si(CH_3)F_3-Cl^-) = 67$ kJ mol^{-1}. The latter pair of numbers shows substitution of CH_3 for F weakening the Si−Cl^- bond. The experimental determination that $D(SiF_4-Cl^-)$ is less than $D(SiFCl_3-Cl^-) = 115$ kJ mol^{-1}, would indicate that substitution of the three equatorial chlorine ligands with more electronegative fluorine ligands *weakens* the Si−Cl^- bond. Calculations at the MP2/LANL2DZpd level give BDEs at 0 K of $D(SiF_4-Cl^-) = 144$ kJ mol^{-1} and $D(SiFCl_3-Cl^-) = 117$ kJ mol^{-1}. The reasons for the discrepancy between theory and experiment for $D(SiF_4-Cl^-)$ are not known. In comparison, the previously reported values $D(PCl_3-Cl^-) = 90$ kJ mol^{-1} and $D(PF_2Cl-Cl^-) = 99$ kJ mol^{-1} (both fluorides equatorial) are consistent with an increase in BDE upon fluoride substitution.[31]

Bond Dissociation Energy Decomposition. The computationally derived BDEs can be divided into several terms as described in detail previously[59] and given in eqs 3 and 4.

$$\Delta E_{BDE} = \Delta E_{prep} + \Delta E_{int} \quad (3)$$

$$\Delta E_{BDE} = \Delta E_{prep} + \Delta E_{elstat} + \Delta E_{Pauli} + \Delta E_{orbital} \quad (4)$$

ΔE_{prep} is the energy associated with deforming the fragments of interest to their geometries in the molecule/ion.[11,60,61] ΔE_{int}, sometimes called the "snap" bond energy, is the energy of bond cleavage when the products are not allowed to relax to their

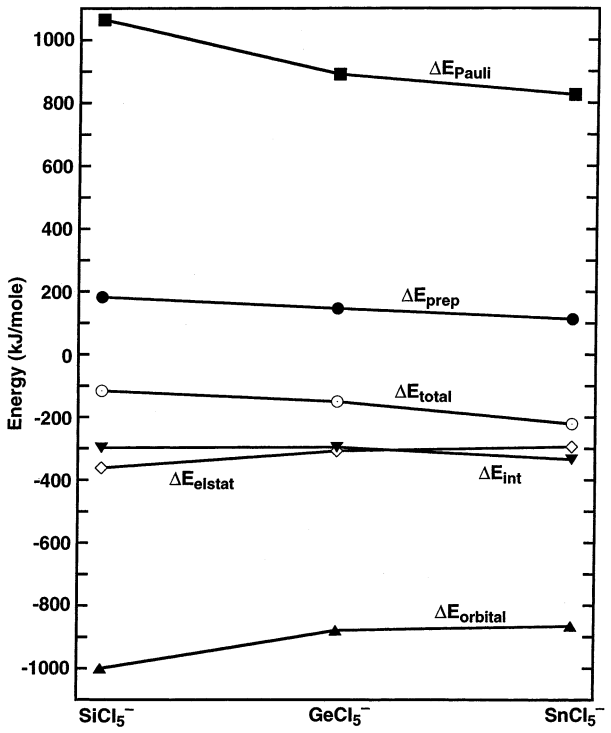

Figure 5. Relative energies (PW91/TZP, kJ mol^{-1}) of the terms in the bond dissociation energy decomposition for the reactions $ACl_5^- \rightarrow ACl_4 + Cl^-$ (A = Si, Ge, Sn).

TABLE 4: Bond Dissociation Energy Decomposition Analysis (kJ mol^{-1})

	E_{total}	E_{prep}	E_{int}	E_{Pauli}	E_{elstat}	$E_{orbital}$
$SiCl_5^-$	−116.2	181.4	−297.6	1063.9	−362.0	−999.6
$GeCl_5^-$	−149.5	146.8	−296.3	890.7	−307.7	−879.3
$SnCl_5^-$	−220.8	113.2	−333.9	825.9	−293.7	−866.1
$Si(CH_3)_3Cl_2^-$	−80.9	123.8	−204.7	712.5	−246.2	−671.0
$Ge(CH_3)_3Cl_2^-$	−102.9	89.8	−192.7	564.5	−196.8	−560.5
$Sn(CH_3)_3Cl_2^-$	−145.9	62.5	−208.4	546.7	−193.0	−562.2
$SiFCl_4^-$	−125.0	161.4	−286.3	1079.0	−364.3	−1001.0
$GeFCl_4^-$	−166.3	126.3	−292.6	888.0	−305.4	−875.2
$SnFCl_4^-$	−237.1	97.9	−335.0	821.8	−293.5	−863.3

equilibrium geometries.[17,31] ΔE_{elstat} is the electrostatic interaction energy between the fragments, ΔE_{Pauli} is the repulsive interaction energy between the fragments resulting from interactions between occupied orbitals, and $\Delta E_{orbital}$ is the energy associated with relaxation of the Kohn−Sham orbitals as self-consistency is reached. ΔE_{elstat} and $\Delta E_{orbital}$ broadly describe electrostatic and covalent attractive aspects of bonding, while ΔE_{Pauli} describes repulsive aspects.

ΔE_{prep} depends on the central atom, the ligands, and the Lewis base. It is calculated to be 200−300 kJ mol^{-1} for $SiCl_4$, depending on the base.[17,61] Fleischer previously attributed the weaker Lewis basicity toward fluoride of SiF_4 compared to GeF_4 to the different calculated ΔE_{prep} values (220 and 155 kJ mol^{-1}, respectively). Clearly, ΔE_{prep} is large enough to dominate the BDE trends. Differences in ΔE_{prep} explain the otherwise surprising fact that $D(PF_3-Cl^-) = 65$ kJ mol^{-1} is weaker than $D(PF_2Cl-Cl^-) = 99$ kJ mol^{-1}.[31]

To assess quantitatively the relative importance of the factors determining the BDEs, the energy decomposition data were derived using the ADF approach described above for the molecules studied experimentally (Table 4). The data appear graphically for the $ACl_5^- \rightarrow ACl_4 + Cl^-$ series in Figure 5. As can be seen in the table, the trends are similar for the $A(CH_3)_3Cl_2^-$ and $AFCl_4^-$ series.

The changes in the values of the terms agree with expectations. (Note that, conventionally, attractive energies are given negative values, such that the BDEs = ΔE_{total} are negative). For example, ΔE_{Pauli} decreases from Si to Sn; the A−Cl bond distances increase, leading to decreased orbital repulsion. Similarly, $\Delta E_{orbital}$ becomes more positive (meaning less orbital interaction between fragments) because the 3p (Ge) and 4p (Sn) orbitals overlap less well with the 2p orbitals of the chloride anion.

The terms ΔE_{Pauli} and $\Delta E_{orbital}$, while large, roughly cancel for each central element, so that the value of ΔE_{int} nearly equals the value of the ΔE_{elstat} term. The trend in the BDE, ΔE_{total}, therefore roughly depends on the sum $\Delta E_{prep} + \Delta E_{elstat}$. The data in Table 4 show that ΔE_{int} hardly changes down the group for the $A(CH_3)_3Cl_2^-$ series. As a consequence, 94% of the difference in ΔE_{total} between Si and Sn arises from the trend in ΔE_{prep}, the energy required to reorganize the chloride ligands on the ACl_4 fragment from trigonal pyramidal to tetrahedral. The more ionic pentachloro and fluorotetrachloro anions show more complex behavior in that ΔE_{int} is similar for Si and Ge, but then changes sizably for Sn. Still, the difference in ΔE_{prep} between $SiCl_5^-$ and $SnCl_5^-$ represents about 65% of the difference in ΔE_{total} between the two, while the percentage for the electronically similar $AFCl_4^-$ series is 57%.

One can view the importance of ΔE_{prep} to the BDE in these systems in the context of ligand repulsions. Steric interactions are related to ΔE_{prep}, which includes the energy costs of moving the ligands in AL_4 closer together to make room for the fifth ligand. Thus, the BDE decomposition analysis includes the effects of ligand−ligand repulsion. The BDE decomposition has the advantage of being computable, while ligand interaction models are easier to understand qualitatively, and are directly related to available geometries.

The ligand close packing (LCP) model emphasizes the effects of ligand−ligand repulsion in systems where the ligands are sufficiently crowded.[62] The van der Waals radii of F and Cl are 1.55 and 1.8 Å;[63] therefore, repulsion is expected for any interaction between fluorine and chlorine atoms closer than 3.35 Å, or two chlorine atoms closer than 3.6 Å. The shortest chlorine−chlorine distances are from axial to equatorial ligands; these distances are given in Table 3. The closest calculated distances in the silicon pentahalide anions are 2.7 and 3.1 Å, respectively. The corresponding values in the tin-containing systems are 3.1 and 3.4 Å, while the germanium values are intermediate. This suggests that there is significant ligand−ligand repulsion in $SiCl_5^-$ and $SiCl_4F^-$, but less in the corresponding germanium and tin ions. These comparisons should be taken in a qualitative sense because of uncertainties in the appropriate van der Waals radii and the precise geometries, as well as corrections for the atomic charge and the angular dependence of the van der Waals radii.[64,65]

The many experimental examples of Cl−Cl distances below 3.6 Å[66] indicate that the chloride ligand is relatively compressible, but there is a balance between the energy cost of ligand−ligand (and ligand−lone pair) repulsion and stretched covalent bonds. Comparison of the bond lengths in ACl_4 and ACl_5^- indicates that the bond lengths in the five-coordinate species are longer by 0.2 Å (axial) or 0.1 Å (equatorial). The fact that the axial bonds are significantly stretched while the equatorial bonds are only slightly stretched is typical of systems with five electron clouds around the central atom.

The steric interactions of polyatomic ligands such as a methyl group are more complicated than those of single atoms, and it is more appropriate to consider the "cone angle" than a van der

TABLE 5: Calculated Atomic Charges Using B3LYP/LANL2DZpd and the NBO Method

molecule	q_A	q_{Cl}(ax)	q_{Cl}(eq)	q_C(eq)	q_F(ax)	q_F(eq)
$Si(CH_3)_3Cl_2^-$	1.72	−0.67		−0.46		
$Si(CH_3)_2Cl_3^-$	1.59	−0.63	−0.44	−0.45		
$Si(CH_3)Cl_4^-$	1.42	−0.56	−0.42	−0.46		
$SiCl_5^-$	1.25	−0.50	−0.42			
$SiCl_4F^-$	1.58	−0.51	−0.46		−0.70	
$SiCl_3F_2^-$	1.89		−0.49		−0.71	
$SiCl_2F_3^-$	2.22	−0.59				−0.69
$SiClF_4^-$	2.47	−0.63			−0.73	−0.70
$Ge(CH_3)_3Cl_2^-$	1.75	−0.70		−0.45		
$Ge(CH_3)_2Cl_3^-$	1.64	−0.67	−0.48	−0.41		
$Ge(CH_3)Cl_4^-$	1.50	−0.59	−0.45	−0.42		
$GeCl_5^-$	1.35	−0.50	−0.45			
$GeCl_4F^-$	1.65	−0.52	−0.48		−0.70	
$GeCl_3F_2^-$	1.92	−	−0.51		−0.70	
$GeCl_2F_3^-$	2.24	−0.58				−0.70
$GeClF_4^-$	2.46	−0.61			−0.73	−0.71
$Sn(CH_3)_3Cl_2^-$	2.02	−0.74		−0.51		
$Sn(CH_3)_2Cl_3^-$	1.96	−0.70	−0.58	−0.49		
$Sn(CH_3)Cl_4^-$	1.86	−0.64	−0.55	−0.48		
$SnCl_5^-$	1.75	−0.57	−0.54			
$SnCl_4F^-$	2.01	−0.58	−0.56		−0.74	
$SnCl_3F_2^-$	2.25		−0.59		−0.74	
$SnCl_2F_3^-$	2.48		−0.61		−0.75	−0.75
$SnClF_4^-$	2.70	−0.66			−0.77	−0.76

Waals radius. The methyl group has almost the same cone angle as a fluoride ligand, while chloride has a larger angle.[67] (The absolute values depend on the central atom.) Consistent with this, ΔE_{prep} for the $A(CH_3)_3Cl$ moieties is smaller than for the corresponding ACl_4 species by 50−60 kJ mol^{-1}. The weaker bonding in systems with methyl ligands is not a steric effect. Instead, as one can see from the BDE decomposition data in Table 4, ΔE_{int} for the methyl complexes is about 100 kJ mol^{-1} smaller than that for the halide complexes.

Comparing the components of ΔE_{int} for anions of the same central element but different ligands is less clear-cut, because the data for the ACl_5^- and $AFCl_4^-$ ions are similar. Expectations are not entirely met when comparing the data for ACl_5^- and $A(CH_3)_3Cl_2^-$. The methyl-containing anions have less negative $E_{orbital}$ values than the pentachlorides, even though chemical intuition suggests that the A−C bonds would be more covalent than the A−Cl bonds.

Furthermore, the trimethyl complexes exhibit smaller ΔE_{elstat} values than do the pentachlorides, as expected in these "more covalent" complexes, but this is not in keeping with the NBO charges for these systems (Table 5). One sees, for example, that Si in $Si(CH_3)_3Cl_2^-$ is more positively charged than in $SiCl_5^-$. A plausible explanation for this is that the equatorial Cl atoms in $SiCl_5^-$ back-donate lone-pair π-electron density to the central element through hyperconjugation. Negative hyperconjugation, where electron density is donated from halogen lone pairs to adjacent A−X antibonding (σ^*) orbitals,[15,68] can also be used to explain the trends in bond lengths. Ignacio and Schlegel[69] found that negative hyperconjugation from a lone pair on a halogen (X) to an adjacent Si-X σ^* orbital lengthens the acceptor bond in tetravalent silicon-containing species, consistent with the calculated geometries. A−C σ^* orbitals are poor acceptors of hyperconjugation compared to A−Cl σ^* orbitals because of the smaller spatial extent of the carbon valence orbitals. Less hyperconjugation in systems with methyl groups is consistent with greater charge on the central atom.

Atomic Charges. NBO atomic charges, which are given in Table 5, can provide additional insight into the bonding in these systems. Comparing molecules with different central atoms but the same ligands, the germanium atoms have a charge 0.03−0.10 higher than the silicon atoms, while the charges on tin are 0.27−0.40 higher than on germanium. While these atomic charges agree with chemical intuition on the effect of going down the periodic table, they are not consistent with electronegativity scales that assign similar values to Si, Ge, and Sn.[63,70] For example, the Pauling electronegativities of Si, Ge, and Sn are 1.90, 2.01, and 1.96, respectively.[63]

The equatorial chlorides have charges ranging from −0.42 to −0.58, while the charges on the equatorial methyl groups are nearly the same (−0.41 to −0.51). The axial chlorides are somewhat more negatively charged (−0.50 to −0.74). The fluoride ligands all have similar charges, ranging from −0.69 to −0.77. Substitution of fluoride for chloride increases the positive charge on the central atom, as expected. Substitution of methyl groups for chlorides increases the negative charge on the remaining chlorides while increasing the positive charge on the central atom. As mentioned above, this contradicts naive expectations. The electronegativity of the methyl group has been calculated to be 2.3,[63] less than that of Cl or F (3.16 and 3.98).[63]

The atomic charges can be correlated with the BDEs. The attraction between two unit charges of opposite sign is 1390 kJ mol^{-1} divided by the interatomic distance in angstroms. Using the calculated interatomic distances and charges, the interaction energy between the central atom and the axial chlorides in ACl_5^- is 390, 400, and 570 kJ mol^{-1} for A = Si, Ge, and Sn, respectively. These energies are consistent with the BDEs in these systems. However, all three $AFCl_4^-$ systems should have interactions that are stronger by about 100 kJ mol^{-1} because of the higher charge on the central atom. This is not seen in either the overall BDEs or in the ΔE_{elstat} values. Also, both fluoride and methyl substitution increase the charge on the central atom, but the former increases chloride affinities while the latter decreases chloride affinities. Thus, a simplistic interpretation of the BDEs in terms of atomic charges is not effective. Obviously, all of the other electrostatic interactions in both AL_5^- and AL_4 would have to be considered to more accurately account for trends in the BDEs. Nevertheless, the effect of fluoride substitution on the chloride affinities of AL_4 is likely to have a significant electrostatic component.

Conclusions

The gas-phase strengths of the A−Cl$^-$ bonds in ACl_5^-, ACl_4F^-, and $A(CH_3)_3Cl_2^-$ (A = Si, Ge, and Sn) have been determined by measuring thresholds for collision-induced dissociation in a flowing afterglow-tandem mass spectrometer. The experimental BDEs in Ge-containing systems are stronger than in the corresponding Si-containing systems by an average of 40 kJ mol^{-1}. BDEs in the corresponding Sn-containing systems are stronger by a further 70 kJ mol^{-1}. Replacement of the three equatorial chlorides with methyl groups weakens the bonds by an average of 65 kJ mol^{-1}, while replacing one axial chloride with a fluoride strengthens the bonds by an average of 17 kJ mol^{-1}. BDEs determined from calculations using the B3LYP model are systematically lower than, but parallel to, the experimental values. MP2 computational results are in better agreement with experiment. The results are consistent with ligand−ligand repulsion significantly affecting the BDEs. This may be the cause of the differences in the reorganization energies (ΔE_{prep}) for the neutral products, which also correlate well with the experimental BDEs. Electrostatic interactions are clearly significant in these systems but cannot be easily correlated with the full set of BDEs.

Acknowledgment. This material is based upon work supported by the National Science Foundation under Grant No.

9985883. We thank Peter Armentrout, Mary Rodgers, and Kent Ervin for use of the CRUNCH software for data analysis and the NIU Computational Chemistry Laboratory (NIU CCL) for computer usage. The NIU CCL is supported in part by the taxpayers of the State of Illinois and by the U.S. Department of Education, Grant P116Z020095.

Supporting Information Available: Figures 1S−6S, giving appearance curves for $Si(CH_3)_3Cl_2^-$, $SiCl_4F^-$, $GeCl_5^-$, $GeCl_4F^-$, $SnCl_5^-$, and $Sn(CH_3)_3Cl_2^-$, and Tables S1−S18, giving experimental and calculated frequencies for reactants and products. This material is available free of charge via the Internet at http://pubs.acs.org.

References and Notes

(1) Reed, A. E.; Schleyer, P. v. R. *J. Am. Chem. Soc.* **1990**, *112*, 1434−1445.

(2) Norman, N. C. *Periodicity and the P-block Elements*; Oxford University Press: Oxford, England, 1994.

(3) Magnusson, E. *J. Am. Chem. Soc.* **1990**, *112*, 7940−7951.

(4) Damrauer, R.; Burggraf, L. W.; Davis, L. P.; Gordon, M. S. *J. Am. Chem. Soc.* **1988**, *110*, 6601−6606.

(5) Kira, M.; Zhang, L. C. Hypercoordinate Silicon Species in Organic Synthesis. In *Chemistry of Hypervalent Compounds*; Akiba, K., Ed.; Wiley-VCH: New York, 1999; pp 147−170.

(6) Chuit, C.; Corriu, R. J. P.; Reye, C. Structure and Reactivity of Hypercoordinate Silicon Species. In *Chemistry Of Hypervalent Compounds*; Akiba, K., Ed.; Wiley-VCH: New York, 1999. Chuit, C.; Corriu, R. J. P.; Reye, C.; Young, J. C. *Chem. Rev.* **1993**, *93*, 1371−1444.

(7) Levy, C. J.; Puddephatt, R. J. *J. Am. Chem. Soc.* **1997**, *119*, 10127−10136.

(8) Sunderlin, L. S. Hypervalent Bonding in Gas-Phase Anions. In *Advances in Gas-Phase Ion Chemistry*; Adams, N., Babcock, L., Eds.; JAI Press: Greenwich, CT, 2001; Vol. 4.

(9) Spencer, J. N.; Barton, S. W.; Cader, B. M.; Corsico, C. D.; Harrison, L. E.; Mankuta, M. E.; Yoder, C. H. *Organometallics* **1985**, *4*, 394−396. Satchell, D. P. N.; Satchell, R. S. *Chem. Rev.* **1969**, *69*, 251−278.

(10) Kobayashi, S.; Busujima, T.; Nagayama, S. *Chem.—Eur. J.* **2000**, *6*, 3491−3494.

(11) Huggett, P. G.; Manning, K.; Wade, K. *J. Inorg. Nucl. Chem.* **1980**, *42*, 665−673.

(12) Larson, J. W.; McMahon, T. B. *J. Am. Chem. Soc.* **1985**, *107*, 766−773.

(13) More recent work suggests that the higher absolute values on the fluoride affinity scale should be adjusted up by ca. 32 kJ mol^{-1}, and this has been done in the results quoted here. Bogdanov, B.; Peschke, M.; Tonner, D. S.; Szulejko, J. E.; McMahon, T. B. *Int. J. Mass Spectrom.* **1999**, *185*, 707−725. Wenthold, P. G.; Squires, R. R. *J. Phys. Chem.* **1995**, *99*, 2002−2005. Lobring, K. C.; Check, C. E.; Sunderlin, L. S. *Int. J. Mass Spectrom.* **2003**, *222*, 221−227.

(14) Windus, T. L.; Gordon, M. S.; Davis, L. P.; Burggraf, L. W. *J. Am. Chem. Soc.* **1994**, *116*, 3568−3579.

(15) Alkorta, I.; Rozas, I.; Elguero, J. *J. Phys. Chem. A* **2001**, *105*, 743−749.

(16) Becke, A. D. *J. Chem. Phys.* **1993**, *98*, 5648−5652.

(17) Fleischer, H. *Eur. J. Inorg. Chem.* **1991**, *393*−*404.*

(18) Chien, S.-H.; Li, W.-K.; Ma, N. L. *J. Phys. Chem. A* **2000**, *104*, 11398−11402.

(19) Muntean, F.; Armentrout, P. B. *J. Chem. Phys.* **2001**, *115*, 1213−1228.

(20) Armentrout, P. B. *J. Am. Soc. Mass Spectrom.* **2002**, *13*, 419−434.

(21) Armentrout, P. B. *Top. Curr. Chem.* **2003**, *225*, 233−262.

(22) Do, K.; Klein, T. P.; Pommerening, C. A.; Sunderlin, L. S. *J. Am. Soc. Mass Spectrom.* **1997**, *8*, 688−696.

(23) Ervin, K. M.; Armentrout, P. B. *J. Chem. Phys.* **1985**, *83*, 166−189. Rodgers, M. T.; Ervin, K. M.; Armentrout, P. B. *J. Chem. Phys.* **1997**, *106*, 4499−4508.

(24) Nakamoto, K. *Infrared and Raman Spectra of Inorganic and Coordination Compounds Part A: Theory and Applications in Inorganic Chemistry*, 5th ed.; John Wiley & Sons: New York, 1997.

(25) McNair, A. M.; Ault, B. S. *Inorg. Chem.* **1982**, *21*, 2603−2605.

(26) Krishnan, R.; Binkley, J. S.; Seeger, R.; Pople, J. A. *J. Chem. Phys.* **1980**, *72*, 650−654. Clark, T.; Chandrasekhar, J.; Schleyer, P. v. R. *J. Comput. Chem.* **1983**, *4*, 294−301.

(27) Dunning, T. H., Jr. *J. Chem. Phys.* **1989**, *90*, 1007−1023. Kendall, R. A.; Dunning, T. H., Jr.; Harrison, R. J. *J. Chem. Phys.* **1992**, *96*, 6796−6806. Woon, D. E.; Dunning, T. H., Jr. *J. Chem. Phys.* **1993**, *98*, 1358−1371. Wilson, A. K.; Woon, D. E.; Peterson, K. A.; Dunning, T. H., Jr. *J. Chem. Phys.* **1999**, *110*, 7667−7676.

(28) Martin, J. M. L.; Sundermann, A. *J. Chem. Phys.* **2001**, *114*, 3408−3420. Bergner, A.; Dolg, M.; Kuechle, W.; Stoll, H.; Preuss, H. *Mol. Phys.* **1993**, *80*, 1431−1441.

(29) Hay, P. J.; Wadt, W. R. *J. Chem. Phys.* **1985**, *82*, 270−283. Wadt, W. R.; Hay, P. J. *J. Chem. Phys.* **1985**, *82*, 284−298. Hay, P. J.; Wadt, W. R. *J. Chem. Phys.* **1985**, *82*, 299−310.

(30) Check, C. E.; Faust, T. O.; Bailey, J. E.; Wright, B. J.; Gilbert, T. M.; Sunderlin, L. S. *J. Phys. Chem. A* **2001**, *105*, 8111−8116.

(31) Check, C. E.; Lobring, K. C.; Keating, P. R.; Gilbert,T. M.; Sunderlin, L. S. *J. Phys. Chem. A.* **2003**, *107*, 8961−8967.

(32) Robertson, E. G.; McNaughton, D. *J. Phys. Chem. A* **2003**, *107*, 642−650.

(33) Loh, S. K.; Hales, D. A.; Lian, L.; Armentrout, P. B. *J. Chem. Phys.* **1989**, *90*, 5466−5485. Schultz, R. H.; Crellin, K. C.; Armentrout, P. B. *J. Am. Chem. Soc.* **1991**, *113*, 8590−8601.

(34) Frisch, M. J.; Trucks, G. W.; Schlegel, H. B.; Scuseria, G. E.; Robb, M. A.; Cheeseman, J. R.; Zakrzewski, V. G.; Montgomery, J. A., Jr.; Stratmann, R. E.; Burant, J. C.; Dapprich, S.; Millam, J. M.; Daniels, A. D.; Kudin, K. N.; Strain, M. C.; Farkas, O.; Tomasi, J.; Barone, V.; Cossi, M.; Cammi, R.; Mennucci, B.; Pomelli, C.; Adamo, C.; Clifford, S.; Ochterski, J.; Petersson, G. A.; Ayala, P. Y.; Cui, Q.; Morokuma, K.; Malick, A D.; Rabuck, K. D.; Raghavachari, K.; Foresman, J. B.; Cioslowski, J.; Ortiz, J. V.; Baboul, A. G.; Stefanov, B. B.; Liu, G.; Liashenko, A.; Piskorz, P.; Komaromi, I.; Gomperts, R.; Martin, R. L.; Fox, D. J.; Keith, T.; Al-Laham, M. A.; Peng, C. Y.; Nanayakkara, A.; Challacombe, M.; Gill, P. M. W.; Johnson, B.; Chen, W.; Wong, M. W.; Andres, J. L.; Gonzalez, C.; Head-Gordon, M.; Replogle, E. S.; Pople. J. A. Gaussian 98, Revision A.9. Gaussian, Inc.: Pittsburgh, PA, 1998.

(35) Glendening, E. D.; Badenhoop, J. K.; Reed, A. E.; Carpenter, J. E.; Bohmann, J. A.; Morales, C. M.; Weinhold, F. NBO 5.0. Theoretical Chemistry Institute, University of Wisconsin, Madison WI, 2001; http://www.chem.wisc.edu/∼nbo5.

(36) Amsterdam Density Functional program, Division of Theoretical Chemistry, Vrije Universiteit, De Boelelaan 1083, 1081 HV Amsterdam, The Netherlands; http://www.scm.com.

(37) (a) Baerends, E. J.; Ellis, D. E.; Ros, P. *Chem. Phys.* **1973**, *2*, 41−51. (b) Baerends, E. J.; Ros, P. *Chem. Phys.* **1973**, *2*, 52−59.

(38) Ravenek, W. In *Algorithms and Applications on Vector and Parallel Computers*; te Riele, H. J. J., Dekker, T. J., van de Horst, H. A., Eds.; Elsevier: Amsterdam, The Netherlands, 1987.

(39) (a) te Velde, G.; Baerends, E. J. *J. Comput. Chem.* **1992**, *99*, 84−98. (b) Boerrigter, P. M.; te Velde, G.; Baerends, E. J. *Int. J. Quantum Chem.* **1988**, *33*, 87−113.

(40) Versluis, L.; Ziegler, T. *J. Chem. Phys.* **1988**, *88*, 322−328.

(41) Vosko, S. H.; Wilk, L.; Nusair, M. *Can. J. Phys.* **1980**, *58*, 1200−1211.

(42) Perdew, J. P.; Chevary, J. A.; Vosko, S. H.; Jackson, K. A.; Pederson, M. R.; Singh, D. J.; Fiolhais, C. *Phys. Rev. B.* **1992**, *46*, 6671−6687.

(43) Snijders, J. G.; Baerends, E. J.; Ros, P. *Mol. Phys.* **1979**, *38*, 1909−1929.

(44) Van Lenthe, E.; van Leeuwen, R.; Baerends, E. J.; Snijders, J. G. *Int. J. Quantum Chem.* **1996**, *57*, 281−293.

(45) Wiberg, N. *Holleman-Wiberg Inorganic Chemistry*, 1st English ed.; Academic Press: San Diego, CA, 2001.

(46) Mingos, D. M. P. *Essential Trends in Inorganic Chemistry*; Oxford University Press: Oxford, England, 1998.

(47) Macho, C.; Minkwitz, R.; Rohmann, J.; Steger, B.; Wölfel, V.; Oberhammer, H. *Inorg. Chem.* **1986**, *25*, 2828−2835.

(48) Schomburg, D. *J. Organomet. Chem.* **1981,** *221*, 137−141. Schomburg, D.; Krebs, R. *Inorg. Chem.* **1984**, *23*, 1378−1389.

(49) Wells, A. F. *Structural Inorganic Chemistry*, 5th ed.; Clarendon Press: Oxford, England, 1984.

(50) Müller, U.; Siekmann, J.; Frenzen, G. *Acta Crystallogr.* **1996**, *C52*, 330−333.

(51) Jóvári, P.; Mészáros, G.; Pusztai, L.; Sváb, E. *J. Chem. Phys. 2001*, **114**, 8082−8090.

(52) Beagley, B.; McAloon, K.; Freeman, J. M. *Acta Crystallogr.* **1974**, *B30*, 444−449.

(53) Sánchez Márquez, J.; Fernández Núñez, M. *J. Mol. Struct.* **2003**, *624*, 239−249.

(54) Atkins, P.; de Paula, J. *Physical Chemistry*; 7th ed.; Freeman: New York, 2002; Chapter 10.

(55) Marcus, Y. *Biophys. Chem.* **1994**, *51*, 111−127.

(56) Cassol, A.; Magon, L.; Barbieri, R. *Inorg. Nucl. Chem. Lett.* **1967**, *3*, 25−29.

(57) Larson, J. W.; McMahon, T. B. *J. Am. Chem. Soc.* **1984**, *106*, 517−521.

(58) Gordon, M. S.; Davis, L. P.; Burggraf, L. W. *Chem. Phys. Lett.* **1989**, *163*, 371−374.

(59) (a) Diefenbach, A.; Bickelhaupt, F. M.; Frenking, G. *J. Am. Chem. Soc.* **2000**, *122*, 6449−6458. (b) Szilagyi, R.; Frenking, G. *Organometallics* **1997**, *16*, 4807−4815. (c) Ziegler, T. *Can. J. Chem.* **1995**, *73*, 743−761. (d) Ziegler, T. *Chem. Rev.* **1991**, *91*, 651−667. (e) Ziegler, T. in *Metal−Ligand Interactions: from Atoms to Clusters to Surfaces*; Salahub, D. R., Russo, N., Eds. Kluwer: The Netherlands, 1992; pp 367−396.

(60) Exner, K.; Schleyer, P. v. R. *J. Phys. Chem. A* **2001**, *105*, 3407−3416.

(61) Timoshkin, A. Y.; Davydova, E. I.; Sevastianova, T. N.; Suvorov, A. V.; Schaefer, H. F. *Int. J. Quantum Chem.* **2002**, *88*, 436−440.

(62) Robinson, E. A.; Gillespie, R. J. *Inorg. Chem.* **2003**, *42*, 3865−3872.

(63) Huheey, J. E.; Keiter, E. A.; Keiter, R. L. *Inorganic Chemistry*, 4th ed. Harper Collins: New York, 1993.

(64) Badenhoop, J. K.; Weinhold, F. *J. Chem. Phys.* **1997**, *107*, 5422−5432.

(65) Batsanov, S. S. *Russ. J. Gen. Chem.* **2002**, *72*, 1153−1156.

(66) Batsanov, S. S. *J. Mol. Struct.* **1999**, *468*, 151−159.

(67) Tolman, C. A. *Chem. Rev.* **1977**, *77*, 313−348.

(68) Shurki, A.; Hiberty, P. C.; Shaik, S. *J. Am. Chem. Soc.* **1999**, *121*, 822−834.

(69) Ignacio, E. W.; Schlegel, H. B. *J. Phys. Chem.* **1992**, *96*, 5830−5837.

(70) Cotton, F. A.; Wilkinson, G.; Murillo, C. A.; Bochmann, M. *Advanced Inorganic Chemistry*, 6th ed.; John Wiley and Sons: New York, 1999.